Applied Thermal Engineering, Volume 147, 25 January 2019, Pages 602-609
DOI:10.1016/j.applthermaleng.2018.10.113

Kinetic study on lignite char gasification with CO_2 and H_2O in a fluidized bed reactor

Shuai Tong[1], Lin Li[1], Lunbo Duan[1,*], Changsui Zhao[1], Edward John Anthony[2]

1. *Key Laboratory of Energy Thermal Conversion and Control, Ministry of Education, School of Energy and Environment, Southeast University, Nanjing 210096, China*
2. *Centre for Combustion and CCS, School of Energy, Environment and Agrifood, Cranfield University, Cranfield, Bedfordshire MK43 0AL, UK*

*Corresponding author.

E-mail address: duanlunbo@seu.edu.cn (L. Duan).

ABSTRACT

Lignite char gasification experiments in CO_2, H_2O and their mixture were performed in a fluidized bed reactor over the temperature range of 1060K to 1210K. The active sites occupied by different gasifying agents in CO_2/H_2O mixture were separated and the kinetics was analyzed. Results show that the reactivity of gasification increases rapidly as the temperature rises. The average reaction rate in 50%CO_2/50%H_2O mixture is slower than the sum of the reaction rates separately, which indicates that CO_2 and H_2O compete for the same reaction active sites on the char surface. Furthermore, with an increase of temperature, the competition capacity of CO_2 gasification over H_2O gradually increases, as a result, CO_2 gasification occupies more active sites than H_2O when the temperature is higher than 1160K. Calculations of the activation energy in the kinetically controlled region based on the shrinking core model reveal that the activation energies follows the trend: $N_2/CO_2>N_2/H_2O>CO_2/H_2O$.

Key words:
Oxy-fuel
Fluidized bed
Gasification
Active sites
Activation energy

1. Introduction

Oxy-fuel combustion is considered to be one of the most promising technologies for carbon dioxide capture from coal-fired power plants due to the fact that it achieves a high concentration of CO_2 in the flue gas and it allows integrating control of pollutants emission. As a result it has attracted worldwide attention in the last two decades [1-7].Unlike conventional combustion, oxy-fuel combustion uses O_2 mixed with recycled flue gas (mainly CO_2 and H_2O) as oxidizer instead of air, and the CO_2 concentration in the exhaust flue gas is more than 90% after condensation, thus simplifying the CO_2 capture process. According to whether the recycled flue gas is condensed or not, it can be divided into oxy-dry recycle and oxy-wet recycle options, and under the oxy-wet

combustion atmosphere, the concentration of water vapor can reach more than 40% [8-10], which is much higher than that of conventional air combustion, where steam concentrations are in the range of 6-10% when firing high quality coal. That is, the flue gas in conventional air combustion is mainly N_2 (>70%), while it consists primarily of CO_2 and H_2O in oxy-fuel combustion [11,12]. Unlike N_2, both CO_2 and H_2O will react with coal char, especially at high temperature. Furthermore, the co-firing of coal and biomass in FBC systems has also been suggested as way of achieving net CO_2 reductions, and this will be associated with very high H_2O levels [13]. Hence, the influence of these gasification reaction in the combustion process needs further investigation [14]. At the same time, under the same reaction conditions, CO_2 and H_2O have different physical and chemical properties (e.g. diffusion, specific heat capacity and reactivity), which influence the combustion process. Therefore, it is of considerable importance to analyze the effect of gasification reactivities of CO_2 and H_2O for oxy-fuel combustion in fluidized bed systems.

Coal gasification is generally divided into two processes: coal pyrolysis and char gasification. In these two processes, char gasification takes up approximately 70%~90% of the reaction time for the whole process. The gasifying agents for char gasification are generally CO_2 and H_2O and the follow two gasification reaction are important at higher temperatures:

$C+CO_2=2CO$ $\Delta H=173kJ/mol$

$C+H_2O=H_2+CO$ $\Delta H=131kJ/mol$

Many previous studies have been performed to investigate coal char reactivity's, when gasified with a single gas agent (CO_2 or H_2O). Scala [15] explored the gasification of a lignite char with CO_2 and H_2O at 775~900°C at atmospheric pressure in a lab-scale fluidized bed apparatus. The results showed that the reactivity of lignite char towards H_2O in the investigated temperature range was greater than that of CO_2 and these workers proposed kinetic models based on their experimental results. Their results showed that the models were able to correctly predict the experimental evolution for the degree of carbon conversion versus time. It has also been suggested that the structure-related kinetic parameters for the two gasification reactions were the same indicating that CO_2 and H_2O were equally likely to attack the same active sites on the char surface. Wang et al. [16] studied the gasification reactivity of two kinds of char with H_2O in fixed bed. These results showed that the reaction occurred mainly in char pores above 0.6nm. Dutta et al. [17] studied the gasification of two kinds of coal and four kinds of char with CO_2 in the thermogravimetric analyzer and this work suggested that the gasification reaction mainly occurred on the surface of pores of 1.5nm or greater. Koba et al. [18] investigated the gasification reactivity of anthracite char and bituminous coal char in CO_2, H_2O, and their mixtures. They found that the gasification rate of H_2O was about 2 to 5 times than that of CO_2.

In practical industrial applications, char gasification with CO_2 and H_2O coexists in many cases. Chen et al. [19] investigated the effect of pyrolysis on the gasification characteristics of lignite char in a mixed atmosphere of CO_2 and H_2O in a thermogravimetric analyzer (TGA) and a fluidized bed and found that the reaction of char with CO_2 was inhibited by H_2O. Wang et al. [20] explored the char gasification reactivity in CO_2/H_2O atmosphere in a modified fixed bed reactor. These results showed that there was a competitive mechanism between the reaction of char with H_2O and CO_2, and H_2O occupied the main active sites. Roberts and Harris [21] used ceramic containers and measured the gasification rates of three Australian bituminous coal chars at elevated pressures. The data showed that the overall reaction rate is not simply the sum of the char reactions with the pure reactants, and that the presence of CO_2 may inhibit the faster char-H_2O reaction. However, they did

not provide direct evidence that common “active sites” assumption is right. On the other hand, Everson et al. [22] found that the reaction rates calculated on the basis of separate active sites assumption fitted their TGA data perfectly. Umemoto et al. [23] studied the gasification characteristics of char in CO_2/H_2O atmosphere in a pressurized drop tube furnace (PDTF) and a TGA at various temperatures. These results showed that H_2O and CO_2 partially shared active sites and they presented a model based on this result, but they had to select some parameters of the model to fit their experimental data. The results discussed above indicate that, although many studies have been published, the question remains: is the net reaction rate lower than the pure gas (CO_2 or H_2O) reaction rate or is it the sum of these reactions when char is gasified within a mixture atmosphere?

The fluidized bed reactor has different heat transfer and mass transfer conditions compared with other reactors, which is important as the heat and mass transfer have an important influence on the gasification reactivity. Therefore, it is important to investigate the gasification reactivity in fluidized bed. Based on the fluidized bed reactor, this paper focuses on the gasification reactivity and kinetics analysis of lignite by analyzing the relationships of reaction rates of char gasification with CO_2, H_2O and their mixture, and quantitatively explores the interaction between CO_2 gasification and H_2O gasification in CO_2/H_2O atmosphere. This work provides important information in future studies of the contribution of gasification reaction to the oxy-fuel combustion in fluidized bed.

2. Experimental

2.1. Samples

Fuel particle size in fluidized bed boiler are generally 0~13 mm. However, large fuel particles are affected by diffusion, while small fuel particles are easily elutriated by fluidized gas. Therefore, a relatively small particle size of test coal (1.25~1.5 mm) was selected to minimize the influence of diffusion, but represent a reasonable choice of particle sizes..

Air-dried samples of Xiaolongtan lignite was used in this work with a size of 1.25~1.5 mm, and the proximate and ultimate analysis of the parent coal are presented in Table 1. The char from the lignite was prepared in a fluidized bed reactor at 1210K under N_2 atmosphere. Once the temperature reached the desires value, the coal samples were fed into the reactor from the feeding port rapidly and the temperature was maintained for 7 min with continuous nitrogen flow, then the electric heating was turned off. After cooling to room temperature, the char samples were separated by screening, the char particles with the size range of about 1~1.2 mm were seleccted. Silica sand (0.3~0.35 mm, 2650 kg/m^3 was used in this experiment with an experimental determined minimum fluidized velocity (u_{mf}) of 0.042 m/s at 1210K), and a static bed height of 0.15 m was employed in these experiments. The fluidized velocity (u_f) was set at 0.126 m/s (u_f/u_{mf} =3), ensuring vigorous bubbling conditions.

Table 1
Proximate and ultimate analysis of Xiaolongtan lignite

Proximate analysis (wt. / %) (as received)				Ultimate analysis (wt. / %) (dry and ash-free basis)				
M	V	A	FC	C	H	O	N	S
16.17	35.53	9.12	39.18	67.11	4.23	25.07	1.45	2.14

2.2. Experimental

In this paper, gasification reaction kinetics analysis is carried out based on a fluidized bed reactor, and the schematic of the experimental setup is given in Fig. 1. The apparatus consists of five major sections: a fluidized bed reactor, gas distribution system, water supply system, temperature control system, and flue gas collection system.

The fluidized bed reactor is divided into upper and lower section (the upper section is the reaction section with the length of 700 mm and the lower section is the preheating section with the length of 500 mm). The two sections are made of quartz glass with inner diameter of 22 mm and length of 1200 mm which heated by an external resistance furnace. A sintered plate is used as the gas distributor.

The gas distribution system is supplied with N_2, CO_2 cylinders, and consists of a high precision injection pump and mass flow control system. The flow rates of CO_2 and N_2 are controlled by two digital mass flowmeters respectively, and the steam flow is accurately controlled by a high precision injection pump. The deionized water is pumped into the preheating section of the FB reactor to generate steam. Steam is carried by N_2 or CO_2. Fluidization gas, premixed in the preheating section, are then used to gasify with coal char in the reaction section. During the experiment, the reaction temperature is continuously controlled within ±5K by a thermocouple inserted into the bed. After the reaction, the exhaust gas is rapidly cooled and dried, then the dried exhaust gas is analyzed by the gas analyzer (Antaris IGS on line Fourier transform infrared multi-component gas analyzer produced by the Thermo Fisher Company of the United States with the resolution of 0.1ppm) constantly.

Prior to testing, several water balance tests are carried out by comparing the amount of water injected into the preheating section with the amount of cooling water in the bottom. Results show that water balance ratios are all over 98% for 2 h. Due to the measurement range of the concentration of each component of exhaust gas by the gas analyzer is limited, 1.2 L/min N_2 is used to dilute the exhaust gas to keep them within reasonable range.

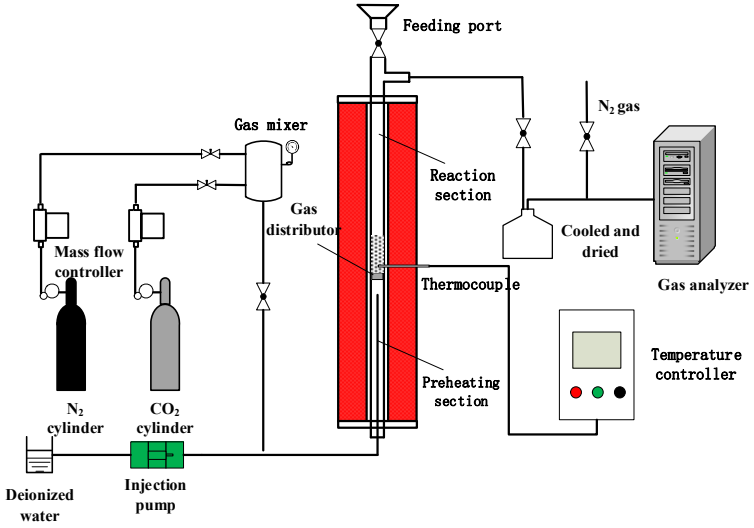

Fig. 1. System diagram of fluidized bed reactor

Prior the start of gasification, the gas analyzer are brought on line and begin analyzing the composition of exhausting flue gas and data is logged by computer. After the concentration of the gas measured in the gas analyzer is stable, then 200±0.5mg char samples (Measured by FA2004

type electronic balance produced by Shanghai Shangping Instrument Company of the China with a resolution of 0.1mg) are rapidly dropped from the feeding port of the reactor. The char samples are rapidly heated to the experimental temperature and char gasification process commences. During gasification experiments, the reactions variable of gasification are determined by the concentration of exhaust gas measured by the gas analyzer, and defined the end of the reaction or not. In order to ensure the reliability of the experimental date, all of these experiments have blank experiments (the same experiments without char particles) to eliminate the influence of the internal and external factors of the experiment system. Also, each experiments is repeated at least 3 times and the only data with good accuracy and repeatability is used. The experimental conditions used for gasification are shown in Table 2. Here 200mg char particles used in the experiment avoid the effect of too low concentration on experimental measurement results.

Table 2

Experimental conditions of gasification

Condition	Temperature *K*	Atmosphere	Condition	Temperature *K*	Atmosphere
1	1060	50%N_2/50%CO_2	7	1160	50%N_2/50%H_2O
2	1110	50%N_2/50%CO_2	8	1210	50%N_2/50%H_2O
3	1160	50%N_2/50%CO_2	9	1060	50%CO_2/50%H_2O
4	1210	50%N_2/50%CO_2	10	1110	50%CO_2/50%H_2O
5	1060	50%N_2/50%H_2O	11	1160	50%CO_2/50%H_2O
6	1110	50%N_2/50%H_2O	12	1210	50%CO_2/50%H_2O

2.3. Methods of data analysis

During the entire gasification procedure, the normalized mass or carbon conversion X is calculated according to:

$$X=\frac{w_0-w_t}{w_0-w_{ash}} \quad (1)$$

Where, w_0 is the initial mass of char samples, w_t is the mass of char at any time and w_{ash} is the mass of the residual ash.

The reaction rate, is defined as the variation of the mass of carbon during the whole reaction time, is given by the following equation:

$$r=\frac{w_0\times C}{t_e} \quad (2)$$

Where, r is the gasification reaction rate, w_0 is the initial mass of char samples, C is the carbon content of the sample particles and t_e is the total time from the start to the end of the reaction.

The peak reaction rate, which is defined as the maximum of carbon conversion rate.

2.4. Kinetic model selection

In numerous kinetic models, the selection of gasification reaction kinetic models is somewhat arbitrary and the decision process complex. Zhang et al. [24] used a typical Chinese anthracite to study gasification under atmospheric pressure and compared the applicability of the volumetric reaction model and shrinking core model according to the reaction parameters. In this work it was found that the shrinking core model describes the anthracite gasification process more accurately, and at the same time, it was also showed that the selection of the models is dependent on the coal

rank. Aranda et al. [25] studied the effect of temperature and partial pressure on the conversion and reactivity of a high-ash coal char gasification with CO_2 and H_2O by using a thermogravimetric analyzer and fluidized bed reactor. Results showed that the experimental data had been fitted to two conversion models (shrinking core model and volumetric reaction model).When coal char was gasified with steam, H_2O molecules could enter the char micropores above 0.6nm of the char, and react at internal and external of the char, thus the volumetric reaction model and shrinking core model were all applicable for coal char gasification with steam. However, when it came to CO_2 gasification, CO_2 molecules could only enter the micropores with diameters larger than 1.5nm, which suggests that it will not react with the internal structure of the char, so CO_2 gasification is better described by a shrinking core model [16,17,23]. In summary, this paper investigates the char gasification reaction kinetics based on the volumetric reaction model and shrinking core model, and then selected the suitable kinetic model ultimately according to the agreement of the results of the model prediction and the experimental results, and hence the kinetic parameters are decided by the selected model.

The first shrinking core model which assumes the reaction occurs at an external surface of the char particle and gradually moves inside, leaving an ash layer to be worn off by the fluidized bed. And it can be expressed as below:

$$\frac{dX}{dt}=k_n P_{CO_2}(1-X)^{\frac{2}{3}} \quad (3)$$

Where X represents the carbon conversion, k_n represents the Knudsen Number, and P_{CO_2} represents the partial pressure of CO_2.

Then the integral of the above equation is obtained:

$$1-(1-X)^{\frac{1}{3}}=\frac{1}{3}k_n P_{CO_2} t \quad (4)$$

Where P_{CO_2} is a constant when reaction gas pressure is fixed, then upper equation becomes:

$$1-(1-X)^{\frac{1}{3}}=kt \quad (5)$$

The second volumetric reaction model, assumes the reaction takes place homogeneously in the volume of the particle and can be expressed as below:

$$\frac{dX}{dt}=k(1-X) \quad (6)$$

Then the integral of the above equation is obtained:

$$-\ln(1-X)=kt \quad (7)$$

The kinetic parameters, k, can all be represented by the Arrhenius equation, as shown below:

$$k=A\exp\left(-\frac{E}{RT}\right) \quad (8)$$

Where, k is the reaction rate constant, E is activation energy, R is molar gas constant, A refers to the pre-exponential factor, and T represents the reaction temperature in eq. (8).

The model fitting method is adopted to calculate kinetic parameters of coal char gasification. Once the mechanism function of reaction kinetic model and reaction rate constant k are determined, then applying the natural logarithm to eq. (8), eq. (9) is obtained. The plot of lnk against $1/T$ fits to a straight line with the activation energy $-E/R$ and pre-exponential factor lnA are obtained from the slope and the intercept respectively.

$$\ln k=\ln A-\frac{E}{RT} \quad (9)$$

3. Results and discussions

3.1. CO/CO_2 concentration and carbon balance

As mentioned above, each of the experiments is repeated at least 3 times, but here we will consider just one of the experimental results as an example in this section. The CO/CO_2 concentration under different reaction conditions are shown in Fig. 2. It is worth noting that the concentration of CH_4 can be measured only in the atmosphere of N_2/H_2O and CO_2/H_2O, and the maximum concentration is never more than 100 ppm. Therefore, the effect of CH_4 on the calculation of carbon balance and carbon conversion can be ignored. It can be seen that with the increase of temperature, the products (CO and CO_2) concentration of gasification increase, the reaction rate is faster and the reaction degree is greater. Coal contains aromatic rings which vary in number and size [26], the carbon bonds in aromatic ring are broken after heating and allow reaction with CO_2 and H_2O to generate CO, H_2 and other products. With an increase of temperature, the carbon bonds are easier to break, which result in better reactivity and a greater degree of reaction [27]. As a result, the carbon conversion increases over the same reaction time. In Fig. 2(a), with the increase of temperature from 1060K to 1210K, the CO concentration increases rapidly and the time from beginning to observing the peak concentration becomes shorter under CO_2 atmosphere. Specifically, here the peak concentration of CO reaches 55000 ppm at 1210K, which is almost twice that seen for 1160K, while the time shortens by a half. In Fig. 2(b), the char gasifies with H_2O to produce CO and H_2 in 50%N_2/50%H_2O atmosphere, then part of CO can be oxidized to CO_2 by H_2O. Here too, the concentration of CO_2 increases along with the increase of temperature. It can be seen in Fig. 2(c) that CO_2 decreases and CO always increases to some degrees with the increase of temperature.

The carbon balance rates are calculated according to the eq. (10):

$$\text{Carbon balance rate}=\frac{\int_0^{te} X_{co}dt+\int_0^{te} X_{co_2}dt}{C}\times 100\% \qquad (10)$$

Where X_{co} and X_{co_2} represent the carbon conversion of CO and CO_2, C is the carbon content of the sample particles and t_e is the total time from the start to the end of the reaction.

The results of carbon balance rates calculation employs only the data with good accuracy (90%~110%), and any data with large errors (<90% or >110%) are discarded. The calculation results of carbon balance rates in different atmospheres and temperatures are shown in Fig. 3. The carbon balance rates are kept in the range of 90%~105% in all the conditions indicating a good measurement accuracy.

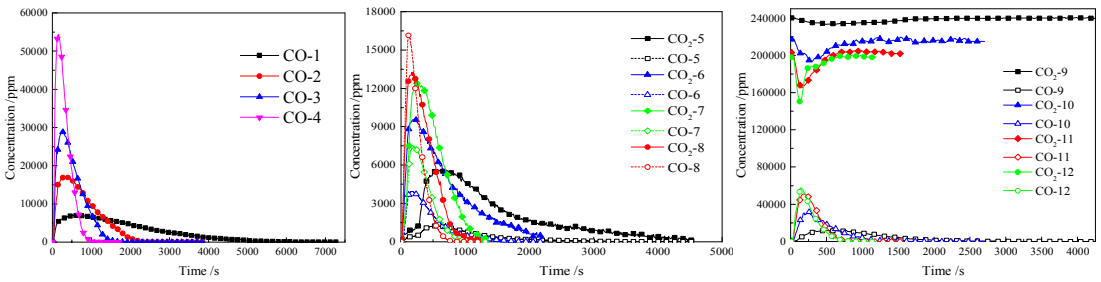

(a) (b) (c)

Fig. 2. Changes of CO and CO_2 concentration versus time in different atmospheres

(a):N_2/CO_2 atmosphere (b):N_2/H_2O atmosphere (c):CO_2/H_2O atmosphere

Note: CO-n and CO_2-n in the figure represent the CO and CO_2 concentration for test condition n

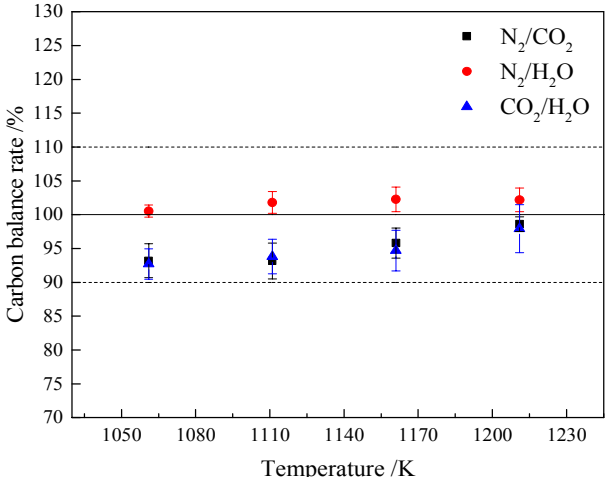

Fig. 3. Carbon balance rate versus temperature in different atmospheres

3.2. Carbon conversion and reaction rate

In order to quantify the reactivity, carbon conversion rate versus time in different atmospheres and temperatures are used and presented in Fig. 4. As mentioned above, data in Fig. 4 are calculated based on the data presented in Fig. 2 which represents just one of the experimental results generated, and is used as an example in this section. Here, the total reaction time, average reaction rate and peak reaction rate are calculated and presented in Fig. 5. Fig. 5(a) and Fig. 5(b) show the total reaction time and average reaction rate versus temperature in different atmospheres, respectively. As expected, with when the temperature increase, the total reaction time decreases and the corresponding average reaction rate increases in all conditions. At the same temperature, the gasification reaction time follows the order: N_2/CO_2>CO_2/H_2O>N_2/H_2O, while the average reaction rate shows the opposite trend. This result is surprising because the reaction rate in CO_2/H_2O atmosphere is even lower than that in N_2/H_2O atmosphere. A possible reason is that CO_2 competes for the same reaction sites with H_2O and blocks the access of H_2O to these sites. As H_2O gasification rate is commonly thought to be one order higher than CO_2 gasification, the competition lowers the total CO_2/H_2O gasification rate. This conclusion is in agreement with Robert et al. [21] who suggested that CO_2 inhibited the faster char-H_2O gasification reaction in the CO_2/H_2O mixture atmosphere. Fig. 5(c) shows the peak reaction rates versus temperature under different atmospheres. Unlike the results discussed above results, the maximum for the peak reaction rates in different temperature both occur in CO_2/H_2O atmosphere in agreement with the results of Chen et al [19].

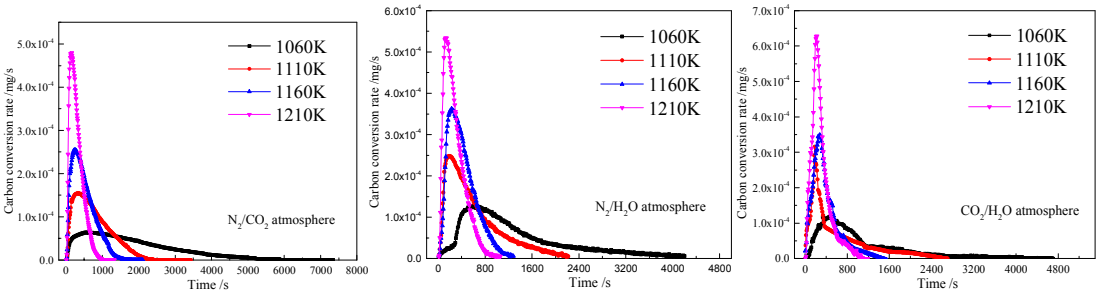

(a) (b) (c)

Fig. 4. Carbon conversion rate versus time in different atmospheres and temperatures

(a): N_2/CO_2 atmosphere (b): N_2/H_2O atmosphere (c): CO_2/H_2O atmosphere

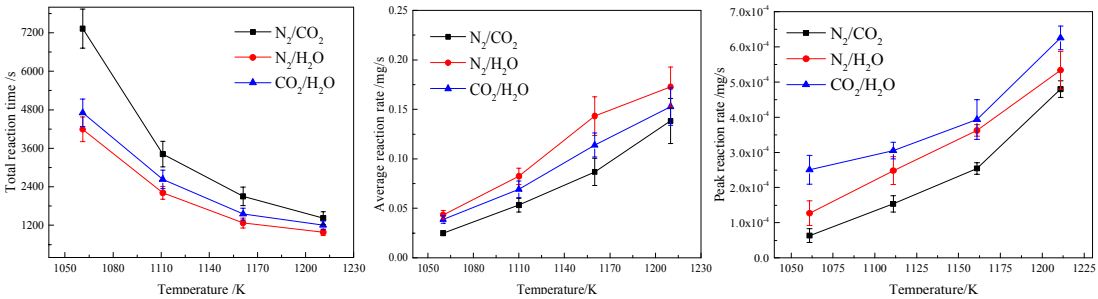

(a) (b) (c)

Fig. 5. The total reaction time, average reaction rate and peak reaction rate versus temperature in different atmospheres

(a): Total reaction time (b): Average reaction rate (c): Peak reaction rate

3.3. Analysis of reaction active sites

As noted, CO_2 and H_2O have different gasification reactivity and compete with each other in CO_2/H_2O mixture atmosphere. Thus, an explanation for the CO_2/H_2O co-gasification mechanism diagram process is presented in Fig. 6: here the area surrounded by black circle in the figure represents all active sites on the char surface; the area surrounded by the blue dashed line in the middle of the figure represents the active sites which CO_2 and H_2O compete with each other. The left area is designated "*a*" which divided by the black curve in the middle of the figure, which represents the active sites occupied by CO_2 while the right area named "*b*" represents the active sites occupied by H_2O on the char surface. What needs to be pointed out is that *a* and *b* are arbitrarily selected.

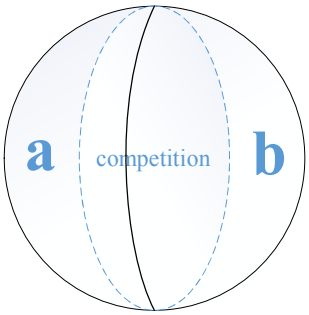

Fig. 6. Conjecture of CO_2/H_2O co-gasification mechanism diagram

In order to analyze the competitive relationship between the reaction active sites of char gasification process in CO_2/H_2O mixture atmosphere, the gasification average reaction rates of char-CO_2, char-H_2O and char-CO_2/H_2O are analyzed. Besides, the interaction of the two kinds of gasification (char-CO_2 and char-H_2O) in CO_2/H_2O mixture atmosphere are also analyzed quantitatively. Assuming in CO_2/H_2O mixture atmosphere, "*m*" is the share of active sites occupied by CO_2 gasification and "*n*" is the share of active sites occupied by H_2O gasification. This can then be it can be formulated as:

$$m + n = 1 \quad (11)$$

Supposing that r_{CO2} is the average gasification reaction rate of char with CO_2 in 50%N_2/50%CO_2 atmosphere, r_{H2O} is the average gasification reaction rate of char with H_2O in 50%N_2/50% H_2O atmosphere and $r_{CO2/H2O}$ is the average gasification reaction rate of char with CO_2

and H_2O in 50%CO_2/50%H_2O mixture atmosphere, respectively. Then:

$$mrco_2 + nr_{H2O}=rco_{2/H2O} \quad (12)$$

According to the measured average gasification reaction rates of char-CO_2, char-H_2O and char-CO_2/H_2O at different temperatures in Fig. 5(b), the share of reaction active sites occupied by CO_2 or H_2O gasification, namely "*m*" and "*n*" at different temperatures can be calculated by combining eq. (11) and eq. (12). The results and errors for the share of active sites are shown in Table 3.

Table 3
Values of the share of gasification *m* and *n*

Temperature / Share	1060 *K*	1110 *K*	1160 *K*	1210 *K*
m	0.2527	0.4584	0.5189	0.5797
n	0.7473	0.5416	0.4811	0.4203
errors	(±0.0018)	(±0.0275)	(±0.0889)	(±0.0849)

The results indicate that the gasification rate is slow and the reactivity is relatively weak at low temperatures (1060K), gasification reaction rate of char with H_2O is faster than that with CO_2, thus H_2O occupies main active sites of char in gasification process. With the increase of temperature, both the CO_2 and H_2O gasification reaction rates increase but the share of active sites occupied by H_2O gasification decreases, while the share of active sites occupied by CO_2 gasification increases correspondingly. The results showed that there may be a compensation effect on reaction active sites when calculating the different active sites occupied by different gasifying agents and the slow gasification reaction rate needed more active sites to accelerate the gasification reaction. Similar conclusions, this is in agreement with the work of Yang et al. [28] who studied the isothermal and non-isothermal char gasification with CO_2 and H_2O by TGA. The reaction rate of char with CO_2 is much slower than that with H_2O and more active sites are needed to speed up the CO_2 gasification. Furthermore, with the increase of temperature, the competition between CO_2 and H_2O becomes more and more evident and the competition capacity of CO_2 gasification over H_2O increases gradually. As a result, CO_2 gasification occupies more active sites than H_2O when the temperature is higher than 1160K.

3.4. Analysis of char gasification kinetics

In order to avoid the influences of the heating process in the early stages and the gas diffusion in the final stages, the carbon conversion *X* in the range of 0.2~0.8 is used as the kinetically controlled region to analyze kinetics of char gasification. As mentioned above, two kinetics models (volumetric reaction model and shrinking core model) are chosen for comparison. The integral format of the models are described in eq. (5) and eq. (7). Fig. 7 displays the modeling results of char gasification which just as an example, where "*S*" and "*V*" represent the shrinking core model and volumetric reaction model and the number "*1*" "*2*" and "*3*" express the experimental atmosphere of N_2/CO_2、N_2/H_2O and CO_2/H_2O, respectively. The fitting coefficients correlations (R^2) of the two models are shown in Table 4. By comparing the modeling results and fitting coefficients, it is found that both of the models are suitable for the experimental data at the range of X=0.2~0.8 for all reaction temperature, but the shrinking core model fits the experimental data better than the volumetric reaction model, which indicates that the shrinking core model can simulate the char

gasification process well in a fluidized bed. Therefore, the shrinking core model is selected as the reaction model for the kinetics analysis in this paper.

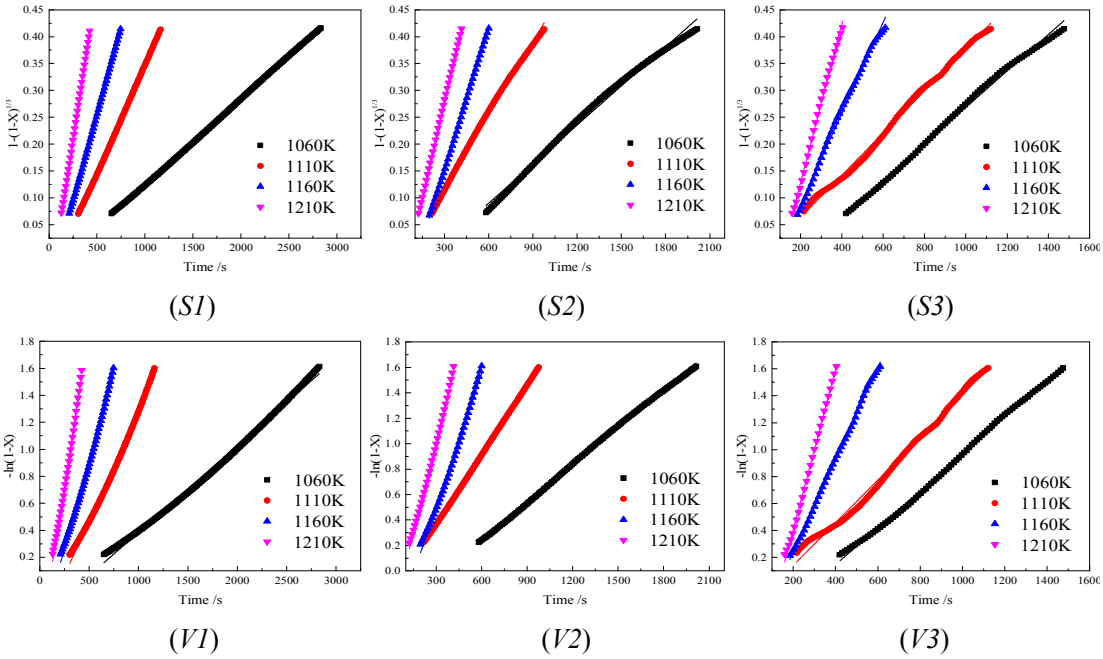

Fig. 7. Modeling results of shrinking core model and volumetric reaction model

Table 4
Correlations for Fitting coefficients of shrinking core model and volumetric reaction model

Model	*S1*				*S2*				*S3*			
T /*K*	1060	1110	1160	1210	1060	1110	1160	1210	1060	1110	1160	1210
R^2	0.999	0.999	0.999	0.999	0.993	0.997	0.999	0.999	0.998	0.996	0.995	0.998
Model	*V1*				*V2*				*V3*			
T /*K*	1060	1110	1160	1210	1060	1110	1160	1210	1060	1110	1160	1210
R^2	0.996	0.995	0.995	0.996	0.999	0.999	0.994	0.997	0.998	0.993	0.999	0.998

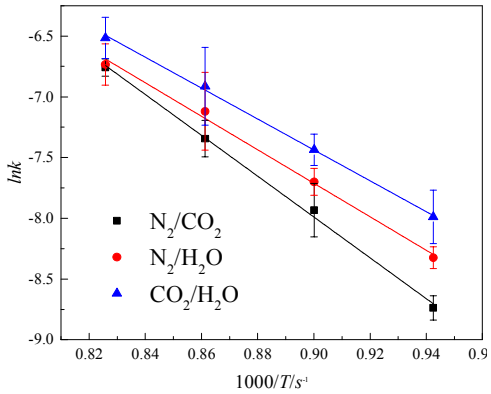

Fig. 8. Fitting results between reaction rate and temperature

According to eq. (9), the fitting results of *lnk* and *1/T* are shown in Fig. 8, the activation energy and pre-exponential factor are represented by the slope and intercept, respectively. The calculation

results of the activation energy and pre-exponential factor are given in Table 5. The results show that the activation energy under different experimental conditions follows the trend: $N_2/CO_2>N_2/H_2O>CO_2/H_2O$. It is generally expected that the higher the activation energy is, the lower the reactivity is, and that the reaction occurs with more difficulty. Thus, the gasification reaction takes place most easily in CO_2/H_2O mixture atmosphere according to the calculation results for the activation energy, which is consistent with the peak reaction rate but is incompatible with the average reaction rate of the whole gasification process. The reasons for these difference are that we just take the carbon conversion X= 0.2~0.8 into consideration when analyzing gasification reaction kinetics, without considering the early and final stages of the reaction. However, during the final stages, the gasification reactivity is relatively low, as a result, the reaction rate is slow and reaction time is long, which can have a strong influence on the average reaction rate. Moreover, due to the ash layer and other factors, the final stages of reaction can experience a strong hindrance to gas diffusion. On the other hand, the gas diffusion rate in CO_2/H_2O atmosphere is slower than that in N_2/H_2O atmosphere under the same condition, and the values of activation energy in CO_2/H_2O and N_2/H_2O atmosphere are fairly close to each other. Therefore, the combination of the above two possible reasons explains the difference between the results of peak and average reaction rates. It is worth explaining that the activation energy in this experiment is much lower than in many investigations related to coal yield activation energies in the order of 220-280 kJ/mol, possible reasons are that we are trying to minimize the influence of diffusion by take the carbon conversion X= 0.2~0.8 as kinetically controlled region into consideration when analyzing kinetics, although the influence of diffusion cannot be completely avoided.

Table 5
Kinetics parameters of char gasification

Atmosphere	*E (kJ/mol)*	*A (s^{-1})*	R^2
50%N_2/50%CO_2	139.75	1259.61	0.997
50%N_2/50%H_2O	114.66	109.95	0.993
50%CO_2/50%H_2O	105.75	55.16	0.998

4. Conclusions

The gasification reactivity of char with CO_2, H_2O, and their mixture are determined using a fluidized bed, and the reaction active sites analysis and dynamic calculation have been performed, and our main conclusions are as follows:

(1) The gasification reactivity is enhanced and the carbon conversion rate increases with the increase of temperature. At the same temperature, the average reaction rates follow the trend: 50%N_2/50%H_2O>50%CO_2/50%H_2O>50%N_2/50%CO_2, while the order of peak reaction rates is: 50%CO_2/50%H_2O>50%N_2/50%H_2O>50%N_2/50%CO_2.

(2) The average reaction rate in 50%CO_2/50%H_2O mixture atmosphere is slower than the sum of the rates of char gasification in separate atmospheres at the same temperature, which indicates that CO_2 and H_2O compete for the same reaction active sites on a reacting char surface. Furthermore, with the increase of temperature, the competition capacity of CO_2 gasification over H_2O increases gradually, and as a result, CO_2 gasification occupies more active sites than H_2O when the temperature is higher than 1160K.

(3) The shrinking core model can represent the experimental data better than the volumetric

reaction model. Calculation of the activation energy of the char reaction in the kinetically controlled region based on the shrinking core model reveals that the activation energy follows the trend: $N_2/CO_2>N_2/H_2O>CO_2/H_2O$.

Acknowledgements

This work is financially supported by the National Natural Science Foundation of China (51776039) and the National Key Research and Development Program of China (2016YFE0102500-06-01).

References

[1] L. Duan, H. Sun, C. Zhao, W. Zhou, X. Chen, Coal combustion characteristics on an oxy-fuel circulating fluidized bed combustor with warm flue gas recycle, Fuel 127 (2014) 47-51.

[2] B. J. P. Buhre, L. K. Elliott, C. D. Sheng, R. P. Gupta, T. F. Wall, Oxy-fuel combustion technology for coal-fired power generation, Prog. Energy Combust. 31 (4) (2005):283-307.

[3] L. Duan, C. Zhao, W. Zhou, C. Qu, X. Chen, O_2/CO_2 coal combustion characteristics in a 50kWth circulating fluidized bed, Int. J. Greenh. Gas Con. 5 (4) (2011) 770-776.

[4] Y. Tan, E. Croiset, M. A. Douglas, K. V. Thambimuthu, Combustion characteristics of coal in a mixture of oxygen and recycled flue gas, Fuel 85 (4) (2006) 507-512.

[5] K. Andersson, F. Johnsson, Process evaluation of an 865MWe lignite fired O_2/CO_2 power plant, Energy Convers. Manage. 47 (18) (2006) 3487-3498.

[6] F. Scala, R. Chirone, Fluidized bed combustion of single coal char particles at high CO_2 concentration, Chem. Eng. J. 165 (3) (2010) 902-906.

[7] F. Scala, R. Chirone, Combustion of single coal char particles under fluidized bed oxyfiring conditions, Ind. Eng. Chem. Res. 49 (21) (2010) 11029-11036.

[8] K. Andersson, R, Johansson, S. Hjärtstam, F. Johnsson, L. Bo, Radiation intensity of lignite-fired oxy-fuel flames, Exp. Therm. Fluid Sci. 33 (1) (2008) 67-76.

[9] V. Becher, J. P. Bohn, A. Goanta, H. Spliethoff, A combustion concept for oxy-fuel processes with low recirculation rate–Experimental validation, Combust. Flame 158 (8) (2011) 1542-1552.

[10] H. Liu, Y. Shao, Predictions of the impurities in the CO_2 stream of an oxy-coal combustion plant, Appl. Energy 87 (10) (2010): 3162-3170.

[11] E. Marek, B. Świątkowski, Reprint of "Experimental studies of single particle combustion in air and different oxy-fuel atmospheres", Appl. Therm. Eng. 74 (1-2) (2015) 61-68.

[12] B. Yi, L. Zhang, F. Huang, Z. Mao, C. Zheng, Effect of H_2O on the combustion characteristics of pulverized coal in O_2/CO_2 atmosphere, Appl. Energy 132 (2014) 349-357.

[13] M. Varol, R. Symonds, E. J. Anthony, D. Lu, L. Jia, Y. Tan, Emissions from co-firing lignite and biomass in an oxy-fired CFBC, Fuel Process. Technol. 173 (2018) 126-133.

[14] D. Kim, S. Choi, C. R. Shaddix, M. Geier, Effect of CO_2 gasification reaction on char particle combustion in oxy-fuel conditions, Fuel 120 (1) (2014) 130-140.

[15] F. Scala, Fluidized bed gasification of lignite char with CO_2 and H_2O: a kinetic study, Proc. Combust. Inst. 35 (3) (2015) 2839-2846.

[16] T. Wang, Q. Liu, Pore characteristics of rapid-pyrolysis char, Journal of Fuel Chemistry and Technology 15 (1) (1987) 73-78 (in Chinese).

[17] S. Dutta, C. Y. Wen, R. J. Belt, Reactivity of coal and char. 1. In carbon dioxide atmosphere, Ind. Eng. Chem. Proc. Des. Dev. 16 (1) (1977) 20-30.

[18] K. Koba, S. Ida, Gasification reactivities of metallurgical cokes with carbon dioxide, steam and their mixtures, Fuel 59 (1) (1980) 59-63.

[19] C. Chen, J. Wang, W. Liu, S. Zhang, J. Yin, G. Luo, H. Yao, Effect of pyrolysis conditions on the char gasification with mixtures of CO_2 and H_2O, Proc. Combust. Inst. 34 (2) (2013) 2453-2460.

[20] Y. Wang, D. A. Bell, Competition between H_2O and CO_2 during the gasification of Powder River Basin coal, Fuel 187 (2017) 94-102.

[21] D. G. Roberts, D. J. Harris, Char gasification in mixtures of CO_2 and H_2O: competition and inhibition, Fuel 86 (17) (2007) 2672-2678.

[22] R. C. Everson, H. W. J. P. Neomagus, H. Kasaini, D. Njapha, Reaction kinetics of pulverized coal-chars derived from inertinite-rich coal discards: gasification with carbon dioxide and steam, Fuel 85 (7) (2006) 1076-1082.

[23] S. Umemoto, S. Kajitani, S. Hara, Modeling of coal char gasification in coexistence of CO_2 and H_2O considering sharing of active sites, Fuel 103 (2013) 14-21.

[24] L. Zhang, J. Huang, Y. Fang, Y. Wang, Gasification reactivity and kinetics of typical Chinese anthracite chars with steam and CO_2, Energy Fuel 20 (3) (2006) 1201-1210.

[25] G. Aranda, A. J. Grootjes, C. M. Van der Meijden, A. Ven der Drift, D. F. Gupta, R. R. Sonde, S. Poojari, C. B. Mitra, Conversion of high-ash coal under steam and CO_2 gasification conditions, Fuel Process. Technol. 141 (2016) 16-30.

[26] K. M. Thomas. Coal Structure [M]// Carbon and Coal Gasification. Springer Netherlands 1986 57-92.

[27] J. Wang, F. Li, L. Chang, K. Xie, The structure characteristics and reactivity of Lingwu coal and its macerals in western China, Energy Source Part A 32 (20) (2010) 1869-1877.

[28] Z. Yang, M. Gao, Y. Bai, F. Li, Study of Co-gasification Kinetics of Coal Char with H_2O and CO_2 , Coal Chemical Industry 44 (5) (2016) 51-57 (in Chinese).

A kinetic study on lignite char gasification with CO2 and H2O in a fluidized bed reactor

Tong, Shuai

2018-10-25

Shuai Tong, Lin Li, Lunbo Duan, et al., A kinetic study on lignite char gasification with CO2 and H2O in a fluidized bed reactor. Applied Thermal Engineering, Volume 147, 25 January 2019, Pages 602-609

https://doi.org/10.1016/j.applthermaleng.2018.10.113